

# Chemical and structural characterization of dapoxetine and its cyclodextrin complexes

PhD Thesis

**András Darcsi**

Doctoral School of Pharmaceutical Sciences  
Semmelweis University



Supervisor:

Szabolcs Béni, Ph.D., associate professor

Official reviewers:

Péter Tétényi, Ph.D. assistant professor  
Gyula Tircsó, Ph.D. assistant professor

Head of the Final Examination Committee:

Tamás Török, D.Sc., professor emeritus

Members of the Final Examination Committee:

Pál Perjési, C.Sc., full professor

Gábor Krajsovsky, Ph.D., associate professor

Budapest

2017

# 1 Introduction

Premature ejaculation (PE) is the most common male sexual disorder, and is estimated to affect up to 30% of men worldwide. PE affects men of all ages equally from pubescent to elderly. Despite its high prevalence and well-known adverse effects on men's life quality, only recently has attention been focused on developing therapeutic strategies. As treatment of the condition numerous non-pharmacological (e.g. psychological and behavioral therapy, self-help techniques, mechanical aids) and pharmacological (topical anesthetics, selective serotonin reuptake inhibitors (SSRIs), type 5 phosphodiesterase inhibitors) approaches are in practice. Dapoxetine (Dpx), is a novel short acting selective serotonin reuptake inhibitor that is being developed specifically as an on-demand oral treatment of PE (Figure 1.). Dpx has been approved by the FDA in 2009, and it is now marketed in over 40 countries. The (*S*)-enantiomer of Dpx (Priligy<sup>®</sup>) is also available in Hungary since 2013.

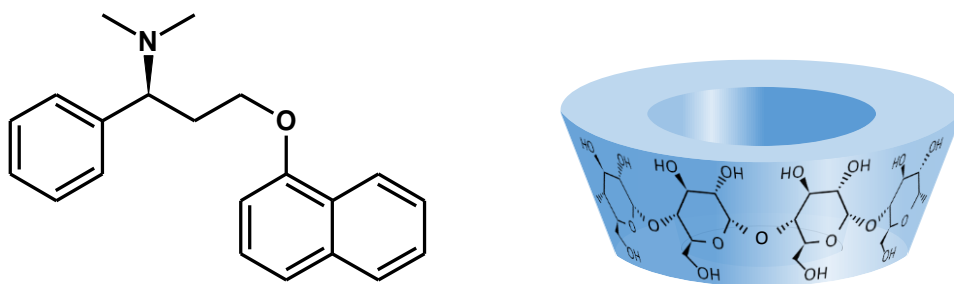


**Figure 1.** The chemical structure of the free base form of (*S*)-dapoxetine and the schematic representation of the native cyclodextrins

Dapoxetine is not yet official in any Pharmacopoeias, therefore literatures describing its chemical and analytical properties are limited. This thesis describes the most important chemical and structural characterization of dapoxetine and its cyclodextrin complexes.

## 2 Objectives

Our aims were to examine the chemical and analytical characterization of Dpx, especially its most commonly used synthetic pathway, degradation process and detailed analytical investigation of Dpx cyclodextrin (CD) complexes.

Therefore, our goals included the isolation, structural characterization and the chemical explanation of the formation of the by-product created in the last step of Dpx synthesis. Further aim was to investigate the degradation process of Dpx which includes the structure elucidation of its degradation products and the description of their formation. Finally, our goal was to conduct a detailed study on Dpx/native CD complexes, using orthogonal analytical techniques (NMR, circular dichroism/UV spectroscopy, mass spectrometry and phase-solubility study). The pH-dependent chiral discrimination properties of a new, single isomer per-carboxymethyl- $\gamma$ -CD derivative (ODMCM- $\gamma$ -CD) were also investigated by NMR and capillary zone electrophoresis, utilizing Dpx and its active metabolites.

## 3 Methods

### 3.1 Phase solubility studies

Phase solubility studies were carried out in a pH 7.40 buffer according to the method described by Higuchi and Connors. Excess amounts of Dpx (1.5 mg) were added to 1 mL solutions with CD concentrations ranging from 1 to 50 mM (for  $\beta$ -CD: 1 to 10 mM). The obtained suspensions were shaken at  $25.0 \pm 0.5$  °C for 24 h. After attaining equilibrium, the samples were centrifuged and the concentration of Dpx was determined spectrophotometrically on a Jasco V-550 instrument at 291 nm.

### 3.2 Mass spectrometry measurements

The accurate mass of the products were determined with an Agilent 6230 time-of-flight (TOF) mass spectrometer. Samples were introduced by the Agilent 1260 Infinity LC system, the mass spectrometer was operated in conjunction with a JetStream (ESI) ion source in positive ion mode. Reference masses of  $m/z$  121.050873 and 922.009798 were used to calibrate the mass axis during analysis. Mass spectra were processed using Agilent MassHunter B.02.00 software.

### 3.3 Nuclear magnetic resonance spectroscopy measurements

The majority of NMR experiments were carried out in D<sub>2</sub>O at 25 °C on a 600 MHz Varian DDR NMR spectrometer (Agilent Technologies, Palo Alto, CA, USA) of the Semmelweis University, equipped with a 5 mm inverse-detection gradient (IDPFG) probehead. Standard pulse sequences and processing routines available in VnmrJ 3.2C/Chempack 5.1 were used. The complete resonance assignments of the Dpx or the CDs was achieved direct <sup>1</sup>H–<sup>13</sup>C, long-range <sup>1</sup>H–<sup>13</sup>C, and scalar spin-spin connectivities, derived from 1D <sup>1</sup>H, <sup>13</sup>C, 2D gCOSY, zTOCSY or ROESY, <sup>1</sup>H,<sup>13</sup>C-gHSQCAD or gHMBCAD (<sup>n</sup>J<sub>CH</sub> = 8 Hz) experiments, respectively. The <sup>1</sup>H chemical shifts were referenced to TMS (0.00 ppm) or the applied NMR solvent CD<sub>3</sub>OD (δ (CD<sub>2</sub>HOD) = 3.310 ppm) and 49.00 ppm for <sup>13</sup>C or CDCl<sub>3</sub> (δ (CHCl<sub>3</sub>) = 7.260 ppm) and 77.160 ppm for <sup>13</sup>C. <sup>1</sup>H chemical shifts in all D<sub>2</sub>O (without DSS) experiments were referenced to the methyl resonance (δ = 3.32 ppm) of internal CH<sub>3</sub>OH present in 20 μM concentration.

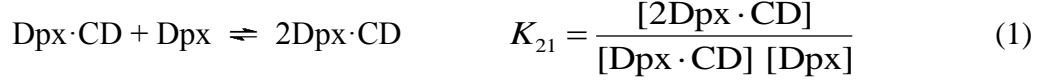
#### 3.3.1 Job's method of continuous variation

The <sup>1</sup>H NMR titration of Dpx according to Job's method was conducted in unbuffered acidic (40 mM CD<sub>3</sub>COOD) D<sub>2</sub>O solutions at 25 °C. The total molar concentration of the two components was kept constant at 3 mM, but the mole fraction of Dpx,  $x_{\text{Dpx}} = c_{\text{Dpx}} / (c_{\text{Dpx}} + c_{\text{CD}})$  was varied gradually in 0.1 unit steps from 0.0 to 1.0. <sup>1</sup>H chemical shifts  $\delta^{\text{Dpx},i}$  were recorded for several (*i*th) Dpx protons and for those exhibiting a monotonic displacement  $\Delta\delta^{\text{Dpx},i} = \delta^{\text{Dpx},i} - \delta_{\text{Dpx}}^i$  with respect to the  $\delta_{\text{Dpx}}^i$  chemical shift of the free component, the absolute values of displacement values  $|\Delta\delta^{\text{Dpx},i}|$  were used to construct the Job's plots. Analogous plots were generated for selected protons of the CD.

#### 3.3.2 <sup>1</sup>H NMR titrations

Since the method of continuous variation does not necessarily provide the best experimental design for stability constant determination, a separate titration was performed under similar circumstances (at 25 °C and in 10 mM CD<sub>3</sub>COOD solution adjusted to pH\* 5.2 with NaOD), but holding  $c_{\text{Dpx}}$  constant and increasing the CD concentration. The 1.0 mM stock solution of Dpx was added to vials containing weighed amounts of CDs (β-CD: 0.1 to 12.0 mM; γ-CD: 0.1 to 25.0 mM) and the mixtures were sonicated and transferred to NMR tubes. The samples were equilibrated for 24 h before acquiring the <sup>1</sup>H NMR spectra.

Our calculation procedure is briefly outlined below for a more complex system, assuming the concurrent formation of  $\text{Dpx} \cdot \text{CD}$  and  $2\text{Dpx} \cdot \text{CD}$  species, denoted hereafter as the  $\{\text{Dpx} \cdot \text{CD}, 2\text{Dpx} \cdot \text{CD}\}$  equilibrium model. Formation of the  $2\text{Dpx} \cdot \text{CD}$  species is described by a second stepwise association constant,  $K_{21}$ :



To evaluate speciation, the equilibrium concentrations  $[\text{CD}]$  and  $[\text{Dpx}]$  are calculated for each titration point from the total concentrations  $c_{\text{CD}}$  and  $c_{\text{Dpx}}$  by solving numerically the nonlinear mass balance equations:

$$c_{\text{CD}} = [\text{CD}] + [\text{Dpx} \cdot \text{CD}] + [2\text{Dpx} \cdot \text{CD}] = [\text{CD}] (1 + K_{11}[\text{Dpx}] + K_{11}K_{21}[\text{Dpx}]^2) \quad (2)$$

$$c_{\text{Dpx}} = [\text{Dpx}] + [\text{Dpx} \cdot \text{CD}] + 2[2\text{Dpx} \cdot \text{CD}] = [\text{Dpx}] (1 + K_{11}[\text{CD}] + 2K_{11}K_{21}[\text{CD}][\text{Dpx}]) \quad (3)$$

The chemical shift ( $\delta^{\text{Dpx},i}$ ) of the  $i$ th carbon-bound measured in each titration point is the weighted average of those in the free  $\text{Dpx}$   $\delta_{\text{Dpx}}^i$  and in the complexes  $\delta_{\text{Dpx} \cdot \text{CD}}^i$  and  $\delta_{2\text{Dpx} \cdot \text{CD}}^i$ ,

$$\delta^{\text{Dpx},i} = \chi_{\text{Dpx}} \delta_{\text{Dpx}}^i + \chi_{\text{Dpx} \cdot \text{CD}} \delta_{\text{Dpx} \cdot \text{CD}}^i + 2\chi_{2\text{Dpx} \cdot \text{CD}} \delta_{2\text{Dpx} \cdot \text{CD}}^i = \frac{\delta_{\text{Dpx}}^i + [\text{CD}](\delta_{\text{Dpx} \cdot \text{CD}}^i K_{11} + \delta_{2\text{Dpx} \cdot \text{CD}}^i 2K_{11}K_{21}[\text{Dpx}])}{1 + [\text{CD}](K_{11} + 2K_{11}K_{21}[\text{Dpx}])} \quad (4)$$

where  $\chi$  denotes molar fraction with respect to the total  $\text{Dpx}$  concentration. If  $\text{CD}$  protons are also monitored during complex formation, similar relationships hold for the observed chemical shift of the  $j$ th  $\text{CD}$  proton,

$$\delta^{\text{CD},j} = \chi_{\text{CD}} \delta_{\text{CD}}^j + \chi_{\text{Dpx} \cdot \text{CD}} \delta_{\text{Dpx} \cdot \text{CD}}^j + \chi_{2\text{Dpx} \cdot \text{CD}} \delta_{2\text{Dpx} \cdot \text{CD}}^j = \frac{\delta_{\text{CD}}^j + \delta_{\text{Dpx} \cdot \text{CD}}^j K_{11}[\text{Dpx}] + \delta_{2\text{Dpx} \cdot \text{CD}}^j K_{11}K_{21}[\text{Dpx}]^2}{1 + K_{11}[\text{Dpx}] + K_{11}K_{21}[\text{Dpx}]^2} \quad (5)$$

where the  $\chi$  molar fractions are normalized to the total  $\text{CD}$  concentration.

Chemical shifts of the free components,  $\delta_{\text{Dpx}}^i$  and  $\delta_{\text{CD}}^j$  can easily be determined from the spectra of  $\text{Dpx}$  or  $\text{CD}$  stock solutions. On the other hand, the chemical shifts specific for the complexes should be iteratively calculated together with the equilibrium constants via computer fitting of functions in Eqs. (4) and/or (5) to the experimental datasets. In the spirit of such a global analysis, input data of our multivariate data evaluation included the total concentrations  $c_{\text{Dpx}}$  and  $c_{\text{CD}}$  for each titration point, known chemical shifts of the free components and the observed chemical shifts of the  $\text{Dpx}$  and  $\text{CD}$  protons most responsive to complexation-induced chemical

shift changes ( $\Delta\delta$ ). The OPIUM computer program was used to perform the least-squares fitting of the model equations like Eqs. (4) and (5) to the datasets in order to determine equilibrium constants as common parameters as well as the complex-specific chemical shifts for each nucleus involved in the calculation. Several stoichiometric models (1:1, 2:1, 1:2 etc.) were tested and besides the chemometric criteria also chemical considerations were used to select the most appropriate equilibrium model (see below). The Hyss program was employed to generate the species distribution plots and the fitted NMR titration curves were generated in Microsoft Excel.

### 3.3.3 NOE type experiments

The average extent of penetration and the direction of inclusion were investigated by nuclear Overhauser effect (NOE) type experiments. 2D ROESY spectra with 512 increments were recorded using a mixing time of 300 ms during a spin-lock of 2.2 kHz.

The interaction of ODMCM- $\gamma$ -CD and racemic Dpx was examined through  $^1\text{H}$ , and 2D ROESY NMR experiments. The NMR solutions were adjusted to pH\* 2.50 and pH\* 7.00, similar to CE experiments. The buffers contained 4 mM ODMCM- $\gamma$ -CD.

## 3.4 Circular dichroism and UV absorption spectroscopic measurements

CD and UV absorption spectra were acquired at  $25 \pm 0.2$  °C on a JASCO J-715 spectropolarimeter equipped with a Peltier thermostat. All spectra were monitored in continuous scanning mode (190-350 nm) at a rate of 100 nm/min, with a step size of 0.2 nm, response time of 1 sec, four accumulations, 1 nm bandwidth, using a 1 cm pathlength quartz cuvette (Hellma, USA).

Circular dichroism and UV spectroscopic titrations of Dpx with  $\beta$ - and  $\gamma$ -CD were performed by successive addition of CD stock solutions (15 and 70 mM) to 1.8 mL aqueous sample of the drug (23 and 30  $\mu\text{M}$ ). JASCO circular dichroism spectropolarimeters record circular dichroism data as ellipticity ( $\Theta$ ) in units of millidegrees (mdeg). The quantity of  $\Theta$  was converted to molar circular dichroic absorption coefficient ( $\Delta\epsilon$  in  $\text{M}^{-1} \text{cm}^{-1}$ ) using the equation  $\Delta\epsilon = \Theta/(33982cl)$ , where, 'c' is the molar concentration of the drug (mol/L), and 'l' is the optical path length expressed in cm.

### 3.5 Molecular modeling

All calculations were performed by the SYBYL 7.2 program (Tripos Inc., St. Louis, MO). The initial geometries of the CDs were based on structures 3CGT and 1P2G in the Brookhaven Protein Database derived from the literature. Initial optimization applied on the structures by MMFF94 force field with 8.0 Å cut-off distance for the non-bonded interactions, 0.7 hydrogen-bond scaling factor and distance dependent dielectric function ( $\epsilon = 78.3$ ), until 0.01 RMS gradient was reached with the BFGS algorithm. According to the energy values of the optimized structures, the lowest energy ones were taken into account for the interaction energies. Structures are visualized by the UCSF Chimera software.

### 3.6 Capillary electrophoresis

All capillary electrophoretic measurements were carried on an Agilent 7100 instrument (Agilent Technologies, Waldbronn, Germany), equipped with a photodiode array detector (DAD) and the Chemstation software for data handling. In the CCE experiments untreated fused silica capillaries were used (50  $\mu$ m id, 58.5 cm total, 50 cm effective length). The temperature of the capillary was set to 20 °C. During measurements 30 kV voltage was applied, UV detection was performed at 200 nm. Samples were injected hydrodynamically (40 mbar  $\times$  3 s). The running buffers were 20 mM phosphoric acid (85%) adjusted to pH 2.5 with 1 M NaOH, and 20 mM NaH<sub>2</sub>PO<sub>4</sub> adjusted to pH 7.0 with phosphoric acid (85%). The BGE contained CDs at various concentrations (1–10 mM) in the chiral screening experiments. The stock solutions of the racemic mixtures of test analytes were prepared in methanol.

## 4 Results

### 4.1 The new process-related impurity of dapoxetine

According to the literature, the last step of the synthesis of Dpx is usually realized through a mesylation reaction (Figure 2.). The advantage of this procedure over other methods is that it also offers the possibility to easily prepare *N*-desmethylated derivatives, the major metabolites of the parent compound. Using methylamine or ammonia in the last step will result in the active metabolites desmethyldapoxetine or didesmethylapoxetine, respectively. Our aim was to isolate (for the first time) the mesylate intermediate for further synthetic purposes.

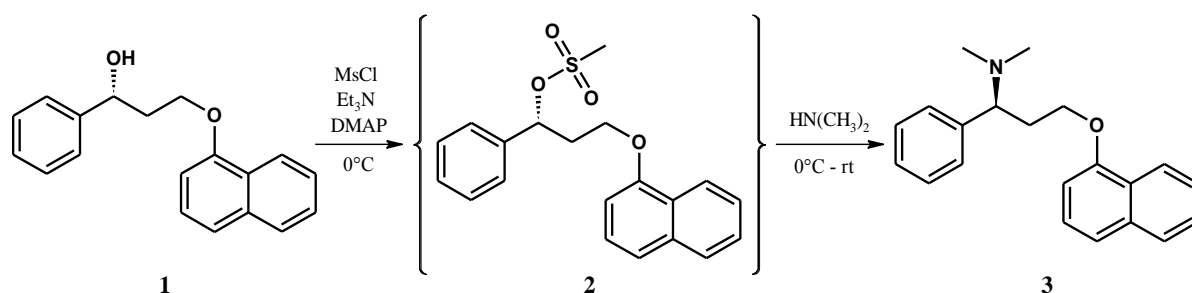


**Figure 2.** Synthetic scheme of dapoxetine involving *in situ* mesylation in the last step

Quenching the mesylation and allowing the reaction mixture to warm up to room temperature resulted in a less polar product compared to the starting material instead of the expected mesylate. The unknown product was isolated by column chromatography and characterized by mass spectrometry (TOF-MS) and various 1D and 2D NMR techniques for structure identification. The complete resonance assignment of the by-product unequivocally proved the formation of the tricyclic 4-phenyl-2H,3H,4H-naphtho[1,2-b]pyran structure.

## 4.2 The new degradation products of dapoxetine

Following the synthesis of Dpx base, the colorless oil turned to brownish yellow upon storage under air atmosphere at room temperature for a few weeks. The purity of Dpx was checked by TLC. Several new UV bands were visualized under UV light, however a major degradation product was observed besides Dpx with a high  $R_f$  value. This major impurity was subjected to isolation and characterization. The NMR resonance assignment of the main degradation product proved the formation of the 1-(2*E*)-cinnamyloxynaphthalene (*E*-CON) structure. Another possibility was the generation of the *Z*-isomer as well, which could arise from the elimination reaction of Dpx. The *cis* arrangement was proven by further NMR techniques.

## 4.3 Characterization of dapoxetine/cyclodextrin interaction

Equilibrium and structural characterization of Dpx cyclodextrins complexes were accomplished by various analytical techniques. 1:1 stoichiometry model was identified from the phase-solubility study, but the 1:2 {Dpx·2CD} complexes were also confirmed in gas phase based on mass spectrometric measurement. The <sup>1</sup>H NMR study of the Dpx/CD interaction was commenced by determining the stoichiometry of association according to Job's method (Figure

3.).  $^1\text{H}$  NMR-based Job's plots and titrations curves undoubtedly prove the simultaneous formation of a  $\{2\text{Dpx}\cdot\text{CD}\}$  complex with both native CD.

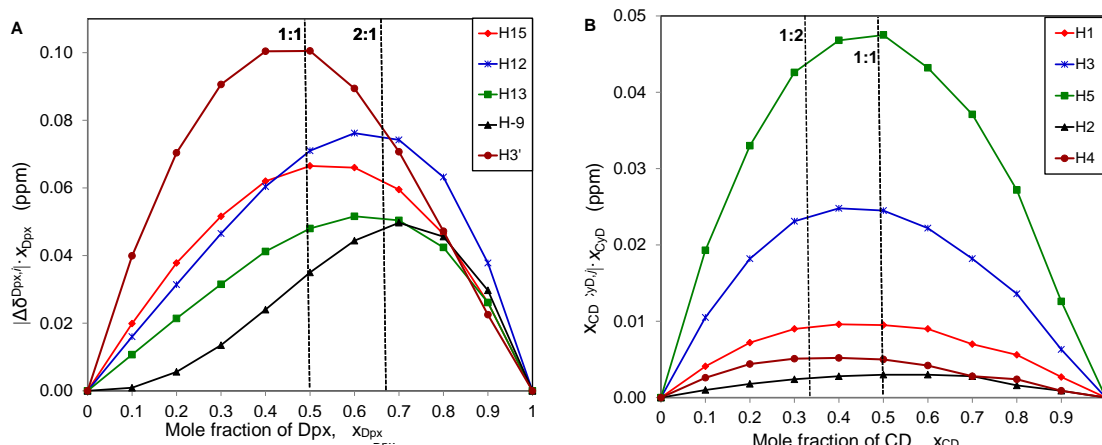


**Figure 3.** Job's plots for selected protons of Dpx (A) and  $\gamma$ -CD (B)

In our case, Job's method of continuous variation and the careful analysis of circular dichroism/UV titrations proved unequivocally that the co-existing complex has the formula  $2\text{Dpx}\cdot\text{CD}$  instead of  $\text{Dpx}\cdot 2\text{CD}$ . To obtain further, atomic-level information on the inclusion geometry, NOE experiments were also carried out supplemented with molecular modelling. The resulting equilibrium constants of Dpx/CD complexes are listed in Table 1.

**Table 1.** Equilibrium association constants [in  $\text{M}^{-1}$ ] of Dpx/CD complexes, obtained in aqueous solution at  $25\text{ }^\circ\text{C}$  by different methods

Complex	Equilibrium constants, measured by				
		phase solubility	$^1\text{H}$ NMR	UV	Circular dichroism
$\text{Dpx}\cdot\beta\text{-CD}$	$K_{11}$	886	915	–	–
$2\text{Dpx}\cdot\beta\text{-CD}$	$K_{21}$	–	276	–	–
$\text{Dpx}\cdot\gamma\text{-CD}$	$K_{11}$	420	661	515	595
$2\text{Dpx}\cdot\gamma\text{-CD}$	$K_{21}$	–	447	–	–
$\text{Dpx}\cdot\text{RAMEG}$	$K_{11}$	594	–	–	–

## 5 Conclusions

### 5.1 The new process-related impurity of dapoxetine

The preparation of the mesylate intermediate was found to be the most crucial step in Dpx synthesis. Our results highlighted, that the conversion of the mesylate strongly depends on the temperature and the presence of the nucleophilic partner, thereby providing different products (Figure 4.).

Increasing the temperature of the reaction mixture in the presence of dimethyl amine favors the formation of Dpx through  $S_N2$  mechanism, while in the lack of the amine the  $S_EAr$  mechanism becomes dominant. Thus, the increase in the temperature results in the competition of the two nucleophilic partners (dimethyl amine and the C2 atom of the naphthyl moiety) influencing the amount of the new pyran impurity.

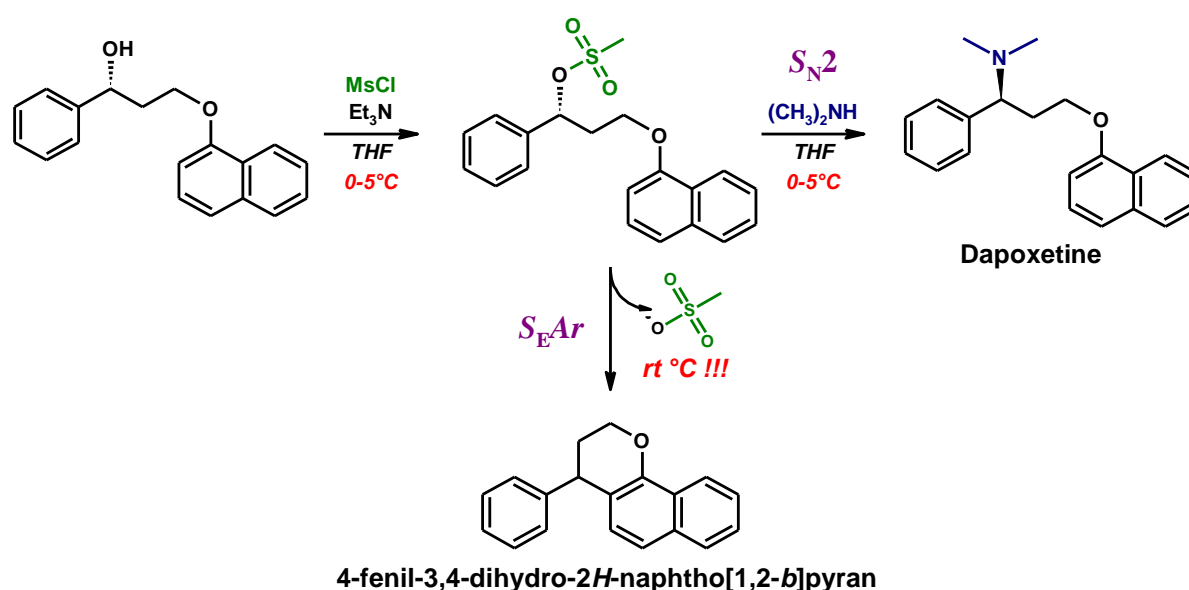


**Figure 4.** The role of temperature and nucleophilicity in the formation of the by-product

Further synthetic possibilities of this reaction were investigated for the synthesis of new heterocyclic compounds.



The new percarboxymethylated  $\gamma$ -CD (ODMCM- $\gamma$ -CD) was successfully applied as a background electrolyte additive in chiral capillary electrophoresis resolving both enantiomers of dapoxetine and its desmethyl derivatives. Dapoxetine showed a pH-dependent inclusion structure with ODMCM- $\gamma$ -CD in which the negatively charged substituents dictate the mode of inclusion (Figure 6.).

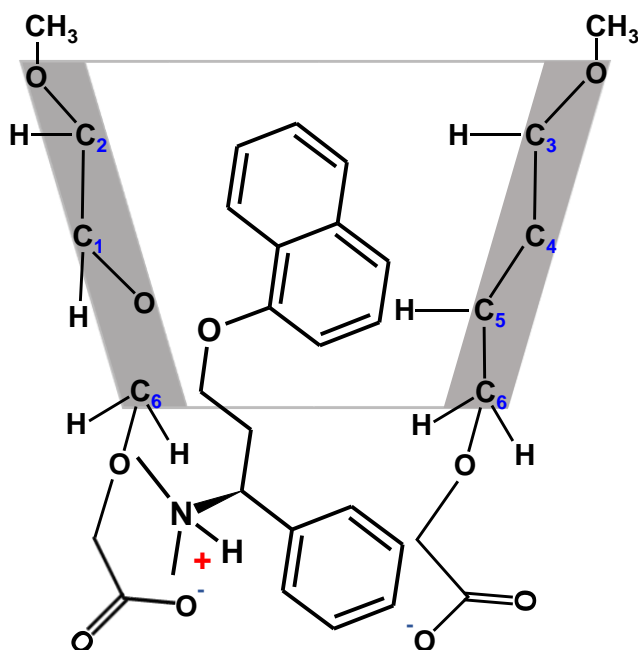


**Figure 6.** The proposed structure for Dpx/ODMCM- $\gamma$ -CD complex based on 2D ROESY NMR measurement at pH 7.0

## 6 Bibliography of the candidate's publication

### 6.1 Publications associated with thesis

1. **Darcsi A**, Rácz Á, Béni S. (2017) Identification and characterization of a new dapoxetine impurity by NMR: Transformation of *N*-oxide by Cope elimination. *J Pharm Biomed Anal*, 134: 187-194.
2. **Darcsi A**, Szakács Z, Zsila F, Tóth G, Rácz A, Béni S. (2016) NMR, CD and UV spectroscopic studies reveal uncommon binding modes of dapoxetine to native cyclodextrins. *RSC Adv*, 6: 102315-102328.
3. **Darcsi A**, Tóth G, Kökösi J, Béni S. (2014) Structure elucidation of a process-related impurity of dapoxetine. *J Pharm Biomed Anal*, 96: 272-277.
4. Benkovics G, Fejős I, **Darcsi A**, Varga E, Malanga M, Fenyvesi É, Sohajda T, Szente L, Béni S, Szemán J. (2016) Single-isomer carboxymethyl- $\gamma$ -cyclodextrin as chiral resolving agent for capillary electrophoresis. *J Chromatogr A*, 1467: 445-453.

### 6.2 Publication related with thesis

5. Neumajer G, Sohajda T, **Darcsi A**, Tóth G, Szente L, Noszál B, Béni S. (2012) Chiral recognition of dapoxetine enantiomers with methylated- $\gamma$ -cyclodextrin: A validated capillary electrophoresis method. *J Pharm Biomed Anal*, 62: 42-47.

### 6.3 Further publications

6. Jankovics P, Lohner S, **Darcsi A**, Németh-Palotás J, Béni S. (2013) Detection and structure elucidation of hydroxythiovaridenafil as an adulterant in a herbal dietary supplement. *J Pharm Biomed Anal*, 74: 83-91.
7. Gampe N, **Darcsi A**, Lohner S, Béni S, Kursinszki L. (2016) Characterization and identification of isoflavonoid glycosides in the root of Spiny restharrow (*Ononis spinosa* L.) by HPLC-QTOF-MS, HPLC-MS/MS and NMR. *J Pharm Biomed Anal*, 123: 74-81.
8. Benkovics G, Hodek O, Havlikova M, Bosakova Z, Coufal P, Malanga M, Fenyvesi É, **Darcsi A**, Béni S, Jindrich J. (2016) Supramolecular structures based on regioisomers of cinnamyl- $\alpha$ -cyclodextrins – new media for capillary separation techniques. *Beilstein J Org Chem*, 12: 97–109.

9. Fejős I, Varga E, Benkovics G, **Darcsi A**, Malanga M, Fenyvesi É, Sohajda T, Szenté L, Béni S. (2016) Comparative evaluation of the chiral recognition potential of single-isomer sulfated beta-cyclodextrin synthesis intermediates in non-aqueous capillary electrophoresis. *J Chromatogr A*, 1467: 454-462.
10. Móricz Á, Ott P G, Häbe T T, **Darcsi A**, Böszörményi A, Alberti Á, Krüzselyi D, Csontos P, Béni S, Morlock G E. (2016) Effect-Directed Discovery of Bioactive Compounds Followed by Highly Targeted Characterization, Isolation and Identification, Exemplarily Shown for *Solidago virgaurea*. *Anal Chem*, 88: 8202-8209.
11. Malanga M, **Darcsi A**, Bálint M, Benkovics G, Sohajda T, Béni S. (2016) New synthetic strategies for xanthene-dye-appended cyclodextrins. *Beilstein J Org Chem*, 12: 537-548.
12. Könye R, Rész Á E, Sólyomváry A, Tóth G, **Darcsi A**, Komjáti B, Horváth P, Noszál B, Molnár-Perl I, Béni S, Boldizsár I. (2016) Enzyme-hydrolyzed fruit of *Jurinea mollis*: a Rich source of (-)-(8R, 8'R)-Arctigenin. *Nat Prod Commun* 11: 1459-1462.